

Solid-State Physics

Contributions by

R. Dornhaus G. Nimtz W. Richter

Spring

; 78

Ergebnisse der exakten Natur

Editor: G. Höhler

Associate Editor: E.A. Niekisch

Editorial Board: S. Flügge J. Hamilton H. Lehmann
G. Leibfried W. Paul

Ralf Dornhaus
Priv.-Doz. Dr. Günter Nimtz

II. Physikalisches Institut, Universität zu Köln, Zülpicher Strasse 77,
D-5000 Köln 41

Dr. Wolfgang Richter

I. Physikalisches Institut, Rheinisch-Westfälische Technische Hochschule Aachen,
Templergraben 55; D-5100 Aachen 1

ISBN 3-540-07774-X Springer-Verlag Berlin Heidelberg New York
ISBN 0-387-07774-X Springer-Verlag New York Heidelberg Berlin

Library of Congress Cataloging in Publication Data. Dornhaus, Ralf. Solid-state physics. Springer tracts in modern physics; 78). Bibliography: p. 1. Semiconductors — Optical properties. 2. Phonons — Scattering. 3. Raman effect. 4. Mercury tellurides. 5. Infra-red detectors. I. Nimtz, Günter, joint author. II. Richter, Wolfgang, joint author. III. Title. IV. Series. QC1.S787. vol. 78. [QC611.6.06]. 539'.08s. [537.6'22]. 76-18956.

This work is subject to copyright. All rights are reserved, whether the whole or part of the material is concerned, specifically those of translation, reprinting, re-use of illustrations, broadcasting, reproduction by photocopying machine or similar means, and storage in data banks. Under § 54 of the German Copyright Law where copies are made for other than private use, a fee is payable to the publisher, the amount of the fee to be determined by agreement with the publisher.

© by Springer-Verlag Berlin Heidelberg 1976.
Printed in Germany.

The use of registered names, trademarks, etc. in this publication does not imply, even in the absence of a specific statement, that such names are exempt from the relevant protective laws and regulations, and therefore free for general use.

Offset printing and bookbinding: Brühlsche Universitätsdruckerei, Giessen.

Contents

The Properties and Applications of the $\text{Hg}_{1-x}\text{Cd}_x\text{Te}$ Alloy System

By *R. Dornhaus* and *G. Nimitz*. With 98 Figures

1. Introduction	1
2. The Crystal	3
2.1 Basic Properties	3
2.2 Phase Diagram and Crystal Growth	5
2.3 Imperfections	7
2.3.1 Dislocations and Native Point-Defects	7
2.3.2 Foreign Atoms	9
3. Band Structure	10
3.1 Band Structure Calculation	11
3.1.1 KKR-Model Calculations	12
3.1.2 Pseudopotential Calculations	15
3.1.3 Tight Binding Model	20
3.2 The Semimetal-Semiconductor-Transition	22
3.3 The Band Edge-Characteristics	23
3.3.1 The Three Level Model of a Small-Gap Semiconductor	23
3.3.2 Statistics	27
3.3.3 Comparison Between Theoretical and Experimental Results	29
3.3.3.1 The Dependence of the Energy Gap E_0 on Composition x , Temperature T and Pressure p	29
3.3.3.2 Effective Masses	31
3.3.3.3 g -Factor of Conduction Electrons	34
3.3.3.4 Higher Interband Energy Gaps	35
3.4 Temperature Dependence of the Band Gap	40
3.5 Pressure Effects on the Band Structure	45
3.6 The Disorder Problem in Pseudo Binary Alloys	48
4. Transport Properties	54
4.1 Hall Coefficient, Intrinsic Carrier Density	54

4.2	Carrier Mobility, Scattering Mechanisms	61
4.3	Magnetoresistance	65
4.4	Magnetic Quantum Effects	69
4.4.1	Shubnikov-de Haas Effect	70
4.4.2	Magnetophonon Effect	73
4.4.3	Cyclotron Resonance	73
4.4.4	Electron-Spin and Combined Resonance	76
4.4.5	Spin-Flip Raman Scattering	78
4.4.6	Various Other Quantum Effects	79
4.5	Hot Carrier Properties	80
4.6	Thermoelectric Effects	82
4.7	Magnetic Susceptibility	84
5.	Optical Properties	86
5.1	Fundamental Reflectivity and Absorption	86
5.1.1	Reflectance and Absorption	86
5.1.2	Magnetorefectance	89
5.1.3	Electroreflectance	89
5.2	Optical Phonons	90
5.3	Free Carrier Absorption and Reflectance	94
6.	Infrared Devices	95
6.1	Recombination Mechanisms and Carrier Lifetime	95
6.2	Photoconductivity	99
6.3	Photovoltaic Effects	101
6.4	Infrared Radiation Sources	103
	Acknowledgements	106
	Notes Added in Proof	106
	List of Important Symbols	109
	Numerical Values of Important Quantities	111
	References	112

Resonant Raman Scattering in Semiconductors

By *W. Richter*. With 54 Figures

1.	Introduction	121
2.	Electric Susceptibility	123
2.1	Direct Transitions	124
2.2	Indirect Transitions	130
2.3	Excitons	131

3. Light Scattering	133
3.1 Scattering Cross Section	133
3.2 Transition Susceptibility (Raman Tensor)	136
3.2.1 Phenomenological Treatment	136
3.2.2 Microscopic Theory	140
3.3 Selection Rules	145
4. Experimental Methods	150
4.1 Apparatus	150
4.1.1 Laser	152
4.1.2 Monochromators	154
4.1.3 Light Detection	155
4.2 Evaluation of Cross Sections	157
4.2.1 The Scattered Power as a Function of the Optical Constants	157
4.2.2 The Determination of the Cross Section and Its Frequency Dependence	164
5. One-Phonon Deformation Potential Scattering	170
5.1 Diamond- and Zincblende-Type Semiconductors	173
5.1.1 Deformation Potentials	177
5.1.2 E_0 -Gap	183
5.1.3 E_1 -Gap	196
5.1.4 E_1 -Gap Under Uniaxial Stress	205
5.2 Wurtzite-Type Materials	213
5.3 Vb-Semiconductors	217
5.4 Vb-Semimetals	221
5.5 Mg_2X -Compounds ($X = Si, Ge, Sn, Pb$)	224
5.6 Other Materials	228
6. Infrared-Active LO Phonons	228
6.1 Fröhlich Interaction	230
6.2 Allowed LO Scattering	232
6.3 Forbidden LO Scattering	233
6.3.1 Forbidden LO Scattering at Fundamental Gaps	234
6.3.2 Forbidden LO Scattering at Higher Gaps	236
7. Multiphonon Scattering	244
7.1 Second-Order Raman Scattering	245
7.2 Microscopic Theory of the Two-Phonon Raman Processes	248

7.3 Two-Phonon Deformation Potential Scattering in Diamond-Zincblende-Type Semiconductors	250
7.3.1 E_0 -Gap	253
7.3.2 E_1 -Gap	255
7.3.3 Evaluation of Two-Phonon Deformation Potentials	258
8. Conclusions	262
Acknowledgements	264
List of Symbols	264
References	267
Subject Index	273

The Properties and Applications of the $\text{Hg}_{1-x}\text{Cd}_x\text{Te}$ Alloy System

Ralf Dornhaus and Günter Nimtz

1. Introduction

This article is concerned with experimental and theoretical studies on the $\text{Hg}_{1-x}\text{Cd}_x\text{Te}$ alloy system. We have attempted to present most of the important published data. However, there were frequent cases where an author cited the references as "to be published" or "private communication" and subsequently missed every opportunity actually to publish such work. Thus we were unable to get all the details of the cited data or get information on their background.

Throughout this article we have endeavoured to use SI units consistently (and where convenient appropriate accepted working units such as "eV" and " cm^{-1} "). Although " m^{-3} " for particle density etc. may be most unpopular with established workers in the field we count on their indulgence and cooperation in eliminating the confusing mixture of units which is still found in the physical literature.

The earliest investigations on the mixed crystal $\text{Hg}_{1-x}\text{Cd}_x\text{Te}$ were aimed at the development of infrared detectors /1/, especially for wavelengths around $10\ \mu\text{m}$ controllable by the composition. This is the region of the second atmospheric window and thus of great interest for communication. It covers also the wavelength of the maximum of thermal radiation at room temperature and could be useful for measuring temperature gradients in the environment or in medical applications. Last not least it straddles the wavelengths of CO_2 -layers. Photodetectors made of this mixed crystal have been working now for more than one decade and have proved themselves the most useful ones for the $10\ \mu\text{m}$ region. They had to compete with other narrow band gap materials, above all with the lead salts. However, crystals of $\text{Hg}_{1-x}\text{Cd}_x\text{Te}$ available nowadays have carrier densities about two orders of magnitude smaller than the lead salts so that their correspondingly larger detectivities more than outweigh the greater difficulty in preparation.

With increasing quality and size of the crystals the HgCdTe alloys attracted the interest of solid state physics. The historical development is similar to that of the classical semiconductors which were used as detectors (with a cat's whisker in the "crystal set" of early radio, and in tens of thousands in the mixer cartridges of wartime microwave radar) long before their basic properties were understood. Today, besides the infrared application, interest centres on phenomena connected with the variation of effective mass and effective g-factor of the conduction band electrons coupled with the variation of the band gap. This shows an approximately linear dependence on the mole fraction x of the components from the positive value for CdTe to the negative one for HgTe. In between there is a composition with zero band gap where according to Kane's theory $m^* \rightarrow 0$ and $g^* \rightarrow \infty$ at the conduction band edge. Crystals close to this composition are, therefore, ideal materials for studying various magnetic quantum and also spin-dependent scattering effects assumed to become more and more pronounced with increasing g-factor which itself represents the spin-orbit interaction. Spin-dependent carrier transport was first observed in magnetic material but is now to be investigated in non-magnetic semiconductors which have a simpler band structure than the magnetic ones. The problem of energy levels of lattice defects in compound semiconductor's such as vacancies and interstitials is also of great interest. As preliminary investigations have shown such defects can generate energy states which interfere with valence band or conduction band states. Various groups are investigating this problem with $\text{Hg}_{1-x}\text{Cd}_x\text{Te}$ alloys, by studying its dependence on the band gap.

In recent years the electronic properties of binary or pseudo-binary alloys have also attracted considerable theoretical interest. The problems of random systems, of which substitutional alloys represent the simplest example, have proved formidable. Many attempts to attack them have been made using a variety of different models. A comparison between experimental and theoretical results may permit a test of different competing theoretical approximations. This may require a reexamination of experimental results, which for lack of a suitable theory have been analysed on the assumption that the alloys were normal crystals. When considering for example the phonon spectrum, alloy scattering or bowing parameters, it has become obvious that the peculiarities of random alloys are important and have to be accounted for in order to obtain a satisfactory theoretical description.

There have been reviews on the $\text{Hg}_{1-x}\text{Cd}_x\text{Te}$ alloy system which have been published during the last few years by LONG and SCHMIT /2/, HARMAN /3/, and HARMAN and MELNGAILIS /4/. They have the emphasis on the photo detector properties rather than transport properties.

The present article is aiming at a fairly complete review of the current state of the art of this alloy system, useful as a basis for future research. It is in

general restricted to compositions with $0 < x < 1$, data of the pure compounds are only given or discussed where those of the mixed crystal are not available.

2. The Crystal

In this chapter the basic physical properties, methods of preparation and imperfections of the $\text{Hg}_{1-x}\text{Cd}_x\text{Te}$ alloy are presented. Some of these properties, for example the elastic or thermal ones, are only known for the pure compounds. However, these data for the pure compounds do not differ markedly so that they represent a good approximation to the values for intermediate compositions, which are not expected to lie outside those for $x = 0$ and $x = 1$.

In the first section the lattice, elastic, thermal, and related properties are given. In the second section the main features of crystal preparation, and in the last section the present knowledge of lattice imperfections are discussed.

2.1 Basic Properties

The $\text{Hg}_{1-x}\text{Cd}_x\text{Te}$ alloy system is formed by II-VI compounds which are isomorphous with zincblende. In the zincblende structure each Te-ion has four nearest neighbours, which in the alloy may be either Hg or Cd. The five possible basic units around a Te-ion site are shown in Fig. 1a. The Brillouin zone of the zincblende lattice is shown in Fig. 1b with the identification of the main symmetry points and lines used throughout this article. It is usually assumed that in the alloy the anions are distributed randomly with a mean density in accordance with the mole fraction x . On the other hand in mixed crystals a trend for clustering, that is to say non-random distribution, has been often observed. In $\text{Hg}_{1-x}\text{Cd}_x\text{Te}$ there is so far no definite experimental proof for such an ordering within a distance of some lattice units. The previously observed splitting of the CdTe reststrahl, discussed in section 5.2, may be a pointer to such a clustering.

The lattice parameters of the compounds HgTe and CdTe are very close to each other, but it was observed by various authors /5,6,7/ that their variation with x is not a linear one (see Fig. 2). This is characteristic for many physical properties of the $\text{Hg}_{1-x}\text{Cd}_x\text{Te}$ alloy as will be seen in later chapters. Fig. 2 includes a plot of the measured density versus composition.

In accordance with the zincblende symmetry ($\bar{4}3m; T_d$) the elastic behaviour is determined by three elastic constants. Published data, available on the pure compounds only, describe approximately the elastic properties of the alloy. As seen in Table 1, the values for the two compounds are within the range of experimental

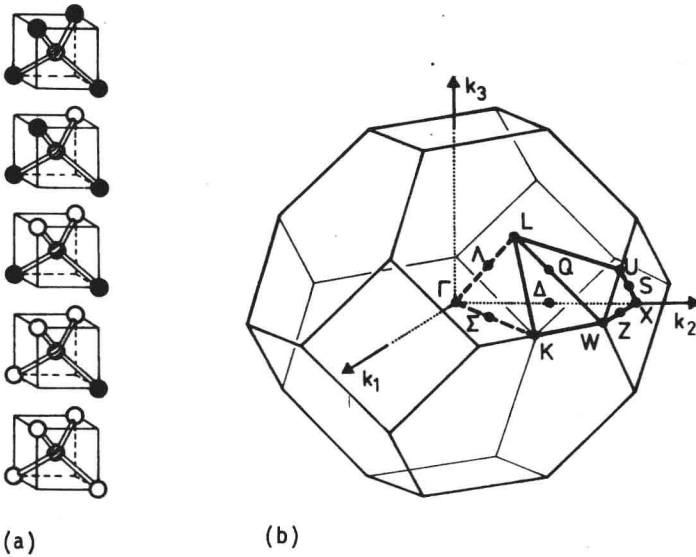


Fig. 1. (a) Basic units of nearest-neighbour ions around a Te-ion site. \circ Hg, \bullet Cd, \ominus Te. (b) Brillouin zone of the zincblende structure

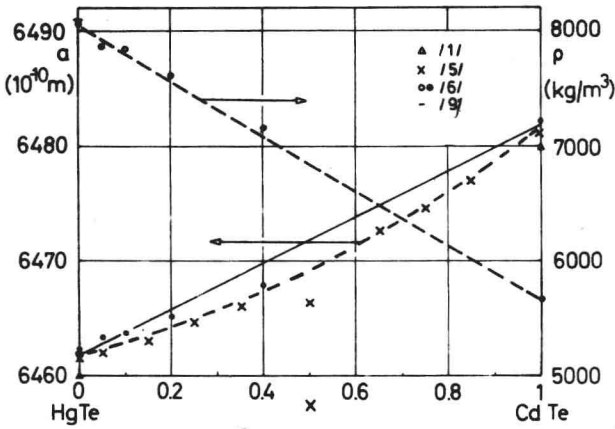


Fig. 2. Lattice parameter a and density ρ for various compositions /1,5,6,9/

error which judging from the scatter of values obtained by different authors seems to be approximately $\pm 10\%$. Sample preparation was reported by ALPER and SAUNDERS /9/ to have an influence of the same order of magnitude. The data of Table 1 are obtained at various temperatures. In the temperature range between 1.4 K and 300 K the elastic constants of HgTe increase with temperature by approximately 8% /9/.

Table 1. Elastic stiffness C, deformation potential D, and piezoelectric constant e

Compound	Ref.	Temp. [K]	C			D _u	D _{u'}	D _d ^C -D _d ^V	e ₁₄ [C/m ²]
			C ₁₁	C ₁₂	C ₄₄				
HgTe	/8/	300	5.08	3.58	2.05				
	/9/	290	5.48	3.81	2.05				
	/9/	4.2	5.92	4.14	2.19				
CdTe	/12/	300	5.35	3.68	1.99	1.77	4.18	-4.5	
	/16/	77	6.15	4.30	1.96			0.0335	

The linear thermal expansion coefficient α of HgTe was investigated by various authors /9-11/. The results show pronounced deviations in the dependence on temperature. For the temperature range between 77 K and 300 K $\alpha \approx 4 \cdot 10^{-6} \text{ K}^{-1}$ appears to be a good approximation.

Preliminary results of the variation of the thermal conductivity with composition have been reported by CHASMAR et al. /13/: they observed a minimum at $x \approx 0.5$. Data on the thermal conductivity and specific heat for $\text{Hg}_{1-x}\text{Cd}_x\text{Te}$, HgTe and CdTe are presented in /14/ and on Debye-Waller factors in /15/.

Crystals with zincblende structure are piezoelectric with one independent component of the piezoelectric tensor. There is no published work on piezoelectric and acoustoelectric effects in the alloy system. The piezoelectric constant e_{14} for CdTe /16/ is listed in Table 1. In the alloy the piezoelectric constant which depends on the ionic charge could vary markedly with composition.

2.2 Phase Diagram and Crystal Growth

In view of two surveys /2,3/ published on this topic during the last few years the main problems and methods will only be reported briefly. Most of the problems in crystal growth of the HgTe-CdTe pseudobinary system arise from the marked difference between the liquidus and solidus curves. A (T,x)-phase diagram is shown in Fig. 3 /17/. The results of the early investigations on the phase diagram /3,6,18/ have shown a large variation between results for both liquidus and solidus lines obtained by different investigations as indicated by the shaded areas in Fig. 3. Determining the (P,T)-phase diagram and the segregation coefficients SCHMIT and SPEERSCHNEIDER /17/ found that the discrepancy is caused by the dependence of the phase transition on the Hg pressure. This pressure dependence is clearly demonstrated for a composition with $x = 0.2$ in Fig. 3, the phase transitions are shifted to lower temperatures when the Hg-pressure is decreased from 2.5 bar to 0.36 bar /17/.

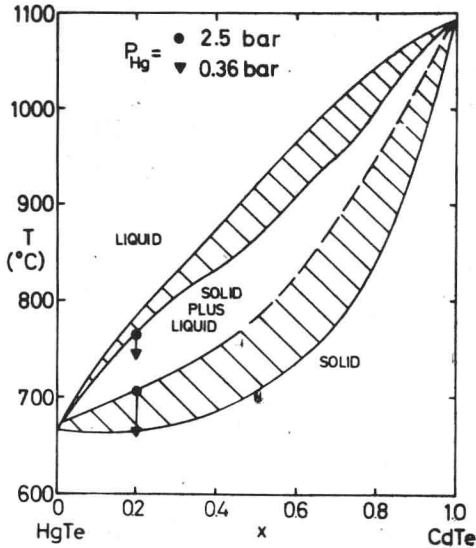


Fig. 3. (T,x) Phase diagram for $\text{Hg}_{1-x}\text{Cd}_x\text{Te}$ /17/. The two pairs of experimental points at $x = 0.2$ demonstrate the influence of mercury pressure on the phase transition

Besides the segregation of CdTe with respect to HgTe there are also problems connected with the segregation of any excess Te in the melt during crystal growth /19/. High quality single crystals of the alloy system have been prepared from ingots either with the three elements or with the two compounds. Growth of crystals by the Bridgman method /2,3,6,19,20/ and by zone melting techniques /21,22/ has been reported. The material as grown, at least in the composition range near $x = 0.2$, is p-type with $10^{22} - 10^{23}$ holes/ m^3 . In a post-crystal-growth annealing process in a Hg atmosphere the crystal can become n-type with electron densities as low as 10^{20} electrons/ m^3 . The mechanism assumed to cause the type inversion is discussed in the following section.

A large number of investigations have been carried out with the preparation of hetero-structures by solid-state diffusion between samples of bulk CdTe and bulk HgTe /23,24/ and by epitaxial growth /25-31/. The epitaxial growth proceeds via evaporation from a HgTe source and the diffusion into a single crystal CdTe substrate. As a result of the interdiffusion of the two compounds on the CdTe substrate, a film with CdTe is grown. The CdTe content decreases with increasing thickness of the condensed film. Thus the films have a graded band gap structure following the variation of composition with thickness. Such structures have been applied as photovoltaic detectors as discussed in section 6.3.

TUFTE and STELZER /30/ have shown that the growth rate and the surface composition of epitaxial layers can be controlled by the use of excess Hg pressure. Recently this effect was studied more extensively by BAILLY et al. /32/ and by SVOB et al. /33/. The experimental results have shown that with increasing Hg

pressure the interdiffusion process between the two compounds is reduced. It is assumed that with increasing Hg pressure the number of vacancies decreases by which the diffusion proceeds /33/. The interdiffusion process was studied also by means of the KIRKENDALL effect /34/.

2.3 Imperfections

Many important physical properties in semiconductors or semimetals such as carrier mobility and carrier density at low temperatures are controlled by imperfections of the crystal. There are three types of imperfection of major interest: dislocations, native point-defects, and foreign atom impurities.

2.3.1 Dislocations and Native Point-Defects

The different types of dislocations in the zincblende structure have been studied by HOLT /35/. One of these, the so-called 60° dislocation was investigated in CdTe. BUCH and AHLQUIST /36/ have shown that this dislocation determines the plastic deformation and acts also as donor or electron trap depending on whether the core of the dislocation is formed by cations or anions in the CdTe compound. So far there is no work available on dislocations in the mixed crystal but there is abundant evidence for native point-defects in the form of vacancies and interstitials. It was soon observed that depending on preparation the samples are n- or p-type. An excess of both types of cations in the crystal yields n-type material, whereas an excess of anion atoms yields p-type material. Thus it is established that free carrier density and carrier type in the extrinsic regime can be controlled by appropriate departures from stoichiometry /2,4,6,17,20,37/. Usually n- or p-type material of $\text{Hg}_{1-x}\text{Cd}_x\text{Te}$ with $x \approx 0.2$ is produced by an annealing process in Hg-rich or Te-rich vapor. It is assumed that three types of defects cause this behaviour, namely Hg and Te vacancies and Hg interstitials. Evidence for Hg vacancies was obtained in semiconducting as well as in semimetallic compositions /38-40/. The Hg vacancy corresponds to an acceptor state, whose energy depends on the mole fraction x , i.e. the band gap as is shown in Fig. 4 /39/. An interesting feature of this acceptor state is that it is resonant with the conduction band for $x < 0.16$. This acceptor state was studied theoretically by MAUGER and FRIEDEL /39/ and by BASTARD and NOZIERES /41/. ELLIOTT et al. /40/ deduced from thermal freeze-out of carriers and from photoluminescence measurements an acceptor level of about 20 meV above the valence band. This energy value was found in semiconducting p-type material with $0.2 \leq x \leq 0.5$. It is sensible to assume this acceptor state also to be related to a Hg vacancy. Pressure dependent measurements of galvanomagnetic transport properties with p-type samples of $x \approx 0.15$ yielded two different acceptor

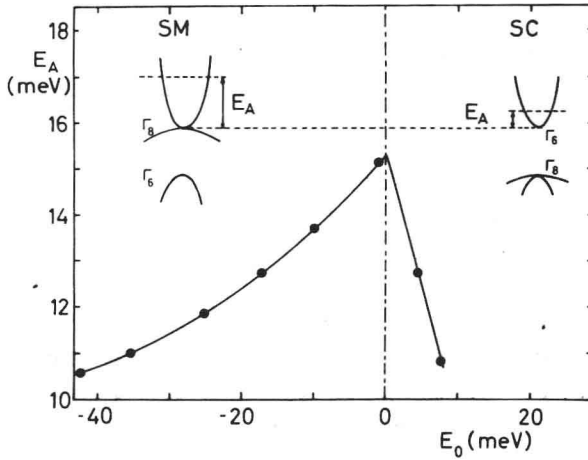


Fig. 4. Acceptor level energy E_A as defined in the insert versus band gap energy /39/

levels /42/. In annealed samples ELLIOTT et al. /42/ could explain the experimental results by an acceptor state 9 meV above the valence band, whereas in as-grown material an acceptor state band of approximately 20 meV above the valence band seems to govern the transport properties.

The infrared emission of hot carriers observed recently /43/ may provide further support to the assumption that a Hg vacancy generates an acceptor state. Comparing the reflectance and the emission spectra which are presented in Figs. 84, 98 it is obvious that in the emission spectrum at the CdTe reststrahl frequency the emission drops to zero but not at the HgTe reststrahl. As described in section 6.4 the p-type layer was obtained by the evaporation of Hg-atoms at the surface of n-type $Hg_{.8}Cd_{.2}Te$. Thus the HgTe sublattice is strongly disturbed and consequently the HgTe reststrahl affected. It is speculated that a high density of Hg vacancies causes the transparency of the surface layer at the HgTe reststrahl frequency /43/.

Hg-rich material was found to be n-type, which may be caused either by Te vacancies or by Hg-interstitials /2,4,6,17,20,37/. From the analysis of various transport effects with n-type $Hg_{.8}Cd_{.2}Te$ DORNHAUS et al. /44/ concluded that the conduction band electrons might be generated by Te vacancies rather than by Hg-interstitials. In the same samples a resonant electronic state was observed in Shubnikov-de Haas experiments and also in the far infrared transmission /45/. The experimental data can be described by an electronic state which is resonant with the conduction band as sketched in the insert of Fig. 5. The energy level of this state is approximately 8 meV above the conduction band at 4.2 K. The absorption coefficient for the transition from conduction band to the resonant level was calculated by analogy with the deuteron photoionization cross section and is compared with experimental data evaluated from transmission measurements in Fig. 5. There are some

theoretical investigations about the states of vacancies in compounds /46-48/ but so far none related to the II-VI compounds which are forming the $Hg_{1-x}Cd_xTe$ alloy.

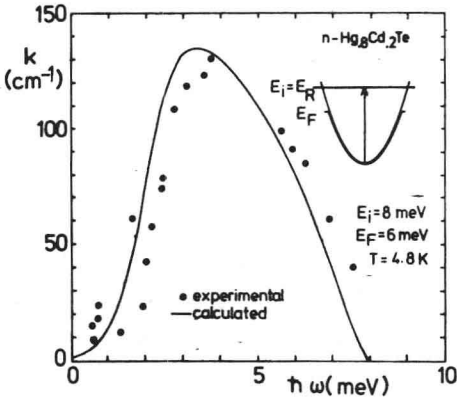


Fig. 5. Absorption coefficient k as deduced from far infrared transmission experiments and as calculated according to the model sketched in the insert /45/

Damage due to proton /4/ and electron irradiation /37,49,50/ can also produce a type conversion. With both proton and electron radiation, the number of electrons was increased and this effect was applied to create n-type layers on p-type bulk material (see chap. 6.3). The defects caused by the radiation are proposed to be either Te vacancies or Hg interstitials /37/. The statistical behaviour of the electron irradiation induced states can be described by two defect levels, as was shown by LEADON and MALLON /50/, one situated in the band gap near the valence band and a second one above the conduction band. Thus the latter is resonant to the conduction band similarly to the state observed by DORNHAUS et al. /45/ which was mentioned above. However, further investigations, both theoretical and experimental, are necessary to give a definite answer on this important question on defects in the $Hg_{1-x}Cd_xTe$ alloy.

2.3.2 Foreign Atoms

For shallow donor and acceptor states in semiconductors the hydrogenic model presents a good approximation /51/. According to this the ionization energy of an impurity E and the Bohr radius a_B is

$$\begin{aligned}
 E &= 13.6 \frac{m_0^*}{m\epsilon_0} \quad (\text{in eV}) \\
 a_B &= 5.29 \cdot 10^{-11} \frac{m\epsilon_0}{m_0^*} \quad (\text{in m})
 \end{aligned}
 \tag{1}$$

in a medium with the band edge effective mass m_0^* and the dielectric constant ϵ_0 . For a composition with $x \approx 0.2$ where m_0^* is small the energy value of a donor state is expected to be only of the order of 1 meV and even at very small impurity densities an overlap of the wavefunctions is expected. Thus a thermal freeze-out of carriers should not occur and the identification of shallow donor states should be rather hard. In semimetallic $\text{Hg}_{1-x}\text{Cd}_x\text{Te}$ the acceptor and donor levels fall into the regions of allowed states of the conduction and valence bands, thus there are acceptor and donor resonance. GEL'MONT and D'YAKONOV /52/ have investigated theoretically this problem. Their study shows that in zero gap materials with a much larger hole than electron effective mass discrete states exist only for the acceptor levels not for the donor levels.

The properties of foreign atoms have been investigated in a number of experiments /3,20,53,54/. However, reliable data are only available for Cu, which acts as acceptor. Its energy level is approximately 1 meV above the Γ_8 band edge in the semimetallic region of the alloy system /41,54/. Donor levels related to foreign atoms have not been identified, which may be caused by the above mentioned small ionization energy expected in the alloy for not too large x values. It can be concluded that in the most widely investigated material the extrinsic transport properties are dominated rather by native point-defects than by foreign impurities. There have been more efforts to obtain and investigate pure materials with a view to technical application and obviously it has been easier to reduce the number of chemical impurities than that of defects.

3. Band Structure

In this chapter we present and discuss band structure calculations and experimental results on band edge characteristics of the mixed II-VI compound $\text{Hg}_{1-x}\text{Cd}_x\text{Te}$. After briefly considering the two components HgTe and CdTe in the first section we deal with three different band structure calculations based on the empirical pseudopotential method, the Korringa-Kohn-Rostocker (KKR)-method and a tight binding approximation.

In the next section we turn to the semimetal-semiconductor-transition in this pseudo binary alloy system, which arises from the fact that HgTe has an inverted band order with a negative fundamental gap $\Gamma_6 - \Gamma_8$ whereas CdTe has standard II-VI bands. In the third section band edge characteristics will be discussed in terms of the Kane model. The next two sections deal with the temperature dependence of the band gap and pressure effects. The last section is concerned with the influence of disorder induced by the statistical distribution of HgTe and CdTe in this mixed crystal.